



LEVEL II

12

14

RADC-TR-80-305

In-House Report

CR-18-80

12 32



AD 8099016

6

MODIFICATION OF THE AN/TRC-97A  
ANTENNA SYSTEM.

15

William G./Mavroides  
Ronald L./Fante

9

*Final rept.*

DTIC  
ELECTE  
MAY 15 1981

16 4600

17 14

E

APPROVED FOR PUBLIC RELEASE; DISTRIBUTION UNLIMITED

ROME AIR DEVELOPMENT CENTER  
Air Force Systems Command  
Griffiss Air Force Base, New York 13441

X NA  
DTIC FILE COPY

309 050

8 1 5 15 008mt

This report has been reviewed by the RADC Public Affairs Office (PA) and is releasable to the National Technical Information Service (NTIS). At NTIS it will be releasable to the general public, including foreign nations.

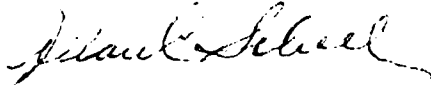
RADC-TR-80-305 has been reviewed and is approved for publication.

APPROVED:



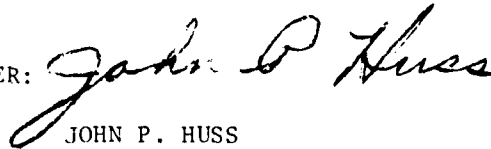
ROBERT J. MAILLOUX, Acting Chief  
Antennas & RF Components Branch  
Electromagnetic Sciences Division

APPROVED:



ALLAN C. SCHELL, Chief  
Electromagnetic Sciences Division

FOR THE COMMANDER:



JOHN P. HUSS  
Acting Chief, Plans Office

**SUBJECT TO EXPORT CONTROL LAWS**

This document contains information for manufacturing or using munitions of war. Export of the information contained herein, or release to foreign nationals within the United States, without first obtaining an export license, is a violation of the International Traffic in Arms Regulations. Such violation is subject to a penalty of up to 2 years imprisonment and a fine of \$100,000 under 22 U.S.C 2778.

Include this notice with any reproduced portion of this document.

If your address has changed or if you wish to be removed from the RADC mailing list, or if the addressee is no longer employed by your organization, please notify RADC ( EEA) Hanscom AFB MA 01731. This will assist us in maintaining a current mailing list.

Do not return this copy. Retain or destroy.

Unclassified

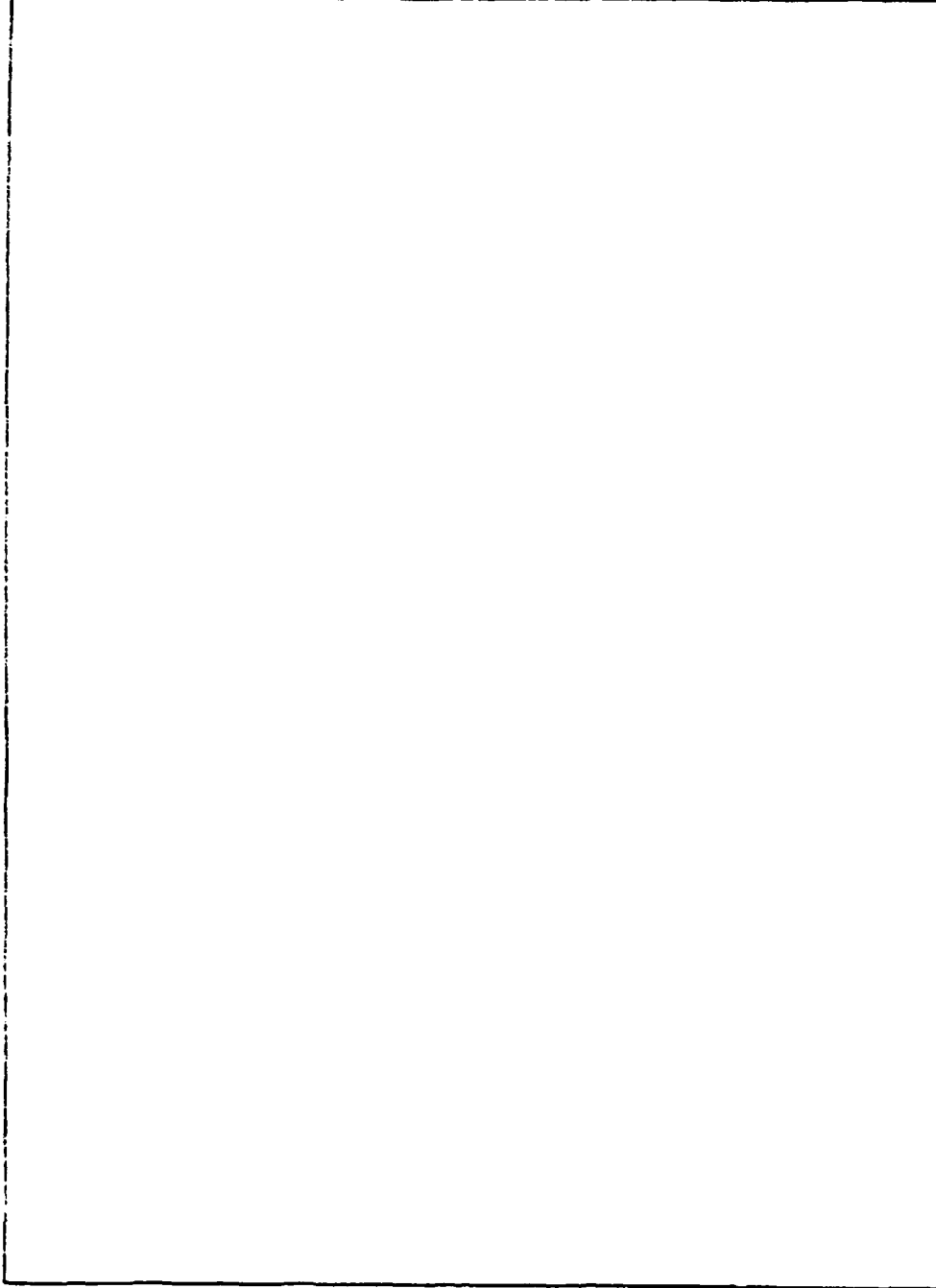
SECURITY CLASSIFICATION OF THIS PAGE (When Data Entered)

REPORT DOCUMENTATION PAGE		READ INSTRUCTIONS BEFORE COMPLETING FORM
1. REPORT NUMBER RADC-TR-80-305 ✓	2. GOVT ACCESSION NO. AD-A099016	3. RECIPIENT'S CATALOG NUMBER
4. TITLE (and Subtitle) MODIFICATION OF THE AN/TRC-97A ANTENNA SYSTEM		5. TYPE OF REPORT & PERIOD COVERED Final Report
		6. PERFORMING ORG. REPORT NUMBER
7. AUTHOR(s) William G. Mavroides Ronald L. Fante		8. CONTRACT OR GRANT NUMBER(s)
9. PERFORMING ORGANIZATION NAME AND ADDRESS Deputy for Electronic Technology (RADC/EEA) Hanscom AFB Massachusetts 01731		10. PROGRAM ELEMENT PROJECT TASK AREA & WORK UNIT NUMBERS 62702F 46001401
11. CONTROLLING OFFICE NAME AND ADDRESS Deputy for Electronic Technology (RADC/EEA) Hanscom AFB Massachusetts 01731		12. REPORT DATE October 1980
		13. NUMBER OF PAGES 32
14. MONITORING AGENCY NAME & ADDRESS (if different from Controlling Office)		15. SECURITY CLASS (of this report) Unclassified
		15a. DECLASSIFICATION/DOWNGRADING SCHEDULE
16. DISTRIBUTION STATEMENT (of this Report)  Approved for public release; distribution unlimited.		
17. DISTRIBUTION STATEMENT (of abstract entered in Block 20, if different from Report)		
18. SUPPLEMENTARY NOTES		
19. KEY WORDS (Continue on reverse side if necessary and identify by block number) Parabolic antennas Antenna sidelobes Aperture illumination Aperture blockage		
20. ABSTRACT (Continue on reverse side if necessary and identify by block number) This report presents the results of an analysis of the AN/TRC-97A tactical troporadio antenna to determine what possible sidelobe reduction can be attained. Theoretical results are presented on the effect of feed and sub-reflector blockage on the radiation patterns. In addition, radiation patterns are included on a modified feed support structure of the existing system which results in improved sidelobes in the azimuth plane.		

DD FORM 1 JAN 73 1473

Unclassified  
SECURITY CLASSIFICATION OF THIS PAGE (When Data Entered)

SECURITY CLASSIFICATION OF THIS PAGE(When Data Entered)



SECURITY CLASSIFICATION OF THIS PAGE(When Data Entered)

Accession For	
DTIC CRA&I	<input checked="" type="checkbox"/>
DTIC TAB	<input type="checkbox"/>
Unannounced	<input type="checkbox"/>
Justification	
Distribution/	
Availability Codes	
Avail and/or	
Dist	Special
A	

### Contents

1. INTRODUCTION	5
2. GENERAL DISCUSSIONS	5
3. THEORETICAL RESULTS	7
4. EXPERIMENTAL INVESTIGATION OF A COMPROMISE ALTERNATIVE	9
5. CONCLUSIONS	14
APPENDIX A: A Study of the Effect of Feed Blockage on the AN/TRC-97A Antenna	15
APPENDIX B: Analysis of the Effect of Subreflector Blockage on the Radiation Pattern of a Cassegrain Modification to the AN/TRC-97A Antenna	25

### Illustrations

1. Original Feedhorn and Waveguide Assembly	6
2. Comparison of the Original AN/TRC-97A Patterns With Ronald L. Fante's Calculations (Vertical polarization)	8
3. Comparison of the Original AN/TRC-97A Patterns With Ronald L. Fante's Calculations (Horizontal polarization)	8
4. Modified Feedhorn and Waveguide Assembly	9

## Illustrations

5.	Comparison of the Original AN/TRC-97A Patterns With the Modified Feed Structure Patterns [Vertical polarization (4.7 GHz)]	11
6.	Comparison of the Original AN/TRC-97A Patterns With the Modified Feed Structure Patterns [Horizontal polarization (4.7 GHz)]	11
7.	Comparison of the Original AN/TRC-97A Patterns With the Modified Feed Structure Patterns [Vertical polarization (4.5 GHz)]	12
8.	Comparison of the Original AN/TRC-97A Patterns With the Modified Feed Structure Patterns [Horizontal polarization (4.5 GHz)]	12
9.	Comparison of the Original AN/TRC-97A Patterns With the Modified Feed Structure Patterns [Vertical polarization (4.9 GHz)]	13
10.	Comparison of the Original AN/TRC-97A Patterns With the Modified Feed Structure Patterns [Horizontal polarization (4.9 GHz)]	13
A1.	Front View of AN/TRC-97A Antenna	16
A2.	Equivalent Model for Blockage by Feed, Waveguides, and Struts	17
A3.	Pattern for Horizontal Polarization in the Horizontal Plane	19
A4.	Pattern for Horizontal Polarization in the Vertical Plane	19
A5.	Pattern for Vertical Polarization in the Horizontal Plane	20
A6.	Pattern for Vertical Polarization in the Vertical Plane	20
A7.	Radiation Pattern of the AN/TRC-97A Reflector (12 dB Edge Illumination)	21
A8a.	Radiation Pattern of the AN/TRC-97A Reflector With Blockage by 5-in. Diameter Circular Feed for Two Different Edge Illuminations	21
A8b.	Radiation Pattern of the AN/TRC-97A Reflector With Blockage by 10-in. Diameter Circular Feed for Two Different Edge Illuminations	22
A9.	Average Sidelobe Levels Due to Reflector Tolerance Errors for Different Correlation Lengths (a)	22
B1.	Geometry of the Modified AN/TRC-97A Antenna	26
B2.	AN/TRC-97A Radiation Pattern With Minimum Blockage Cassegrain Feed and -20 dB Edge Taper	28
B3.	AN/TRC-97A Radiation Pattern With Minimum Blockage Cassegrain Feed and -14 dB Edge Taper	29

## Tables

A1.	Effective Blockage Widths of the Waveguides and Struts at $\lambda = 2.51$ in.	16
-----	--	----

## Modification of the AN/TRC-97A Antenna System

### 1. INTRODUCTION

In response to a request by RADC/DCCT, RADC/EEAA undertook the task of investigating the feasibility of improving the sidelobe structure of the AN/TRC-97A Troposcatter Antennas. The approach taken in this study was to evaluate options that would, in varying degrees, utilize the present reflector and so achieve a system improvement at low cost to the government. The options, ranked in order of increasing complexity and cost are to simply alter the feed horn illumination on the main lens, to reduce or redistribute feed blockage if possible, to use a Cassegrain configuration with a small subreflector for low blockage, and finally to procure an offset reflector antenna with a highly tapered illumination. This report includes theoretical studies in Appendices A and B that address these options, and in addition it presents experimental data of a potentially low cost option that lowers the sidelobes in the azimuth plane at the expense of elevation plane sidelobes.

### 2. GENERAL DISCUSSIONS

Existing AN/TRC-97A Troposcatter Antennas were designed more than ten years ago during an era of modest ECM/ARM capability. Consequently design

---

(Received for publication 3 October 1980)

emphasis on extremely low sidelobe levels, a must in today's ECM environment, was not required. A sketch of the original parabola and feed horn assembly is shown in Figure 1. The sidelobe level in the immediate proximity to the main beam is due to the following:

- (1) Aperture illumination of the reflector by the feed,
- (2) Distortion and/or manufacturing tolerances of the reflector,
- (3) Aperture blockage due to the feed structure.

The wide angle sidelobes are due primarily to spillover energy radiated by the feed and not intercepted by the reflector. No attempt was made in this study to address this problem because of the dominance of the near sidelobes.

The approach taken in this study was to conduct a theoretical investigation coupled with an experimental modification program.

1. Theoretical investigation: to determine
  - (a) Effect of feed blockage,
  - (b) Analysis of sidelobes predicted by a Cassegrain system,
  - (c) Best sidelobe structure possible with other alternatives.
2. Experimental investigations:
  - (a) Redesigning the feed horn,
  - (b) Rerouting existing waveguide runs to reduce the blockage sidelobes in the azimuth plane.

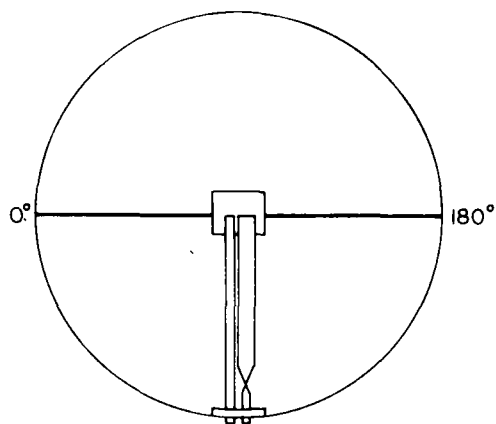


Figure 1. Original Feedhorn and Waveguide Assembly

### 3. THEORETICAL RESULTS

The theoretical investigations were conducted by Ronald L. Fante, and the results presented are in the letter report of 4 January 1980, "A Study of the Effect of Feed Blockage on the AN/TRC-97A Antenna" (see Appendix A) and the letter report of 20 February 1980, "Analysis of the Effect of Subreflector Blockage on the Radiation Pattern of a Cassegrain Modification to the AN/TRC-97A Antenna" (see Appendix B). The results suggest: (1) that changing dish illumination will not significantly reduce the sidelobe levels as the computed data indicate that the primary source of the sidelobes is strut and waveguide blockage; and (2) that because of subreflector blockage it does not appear possible to design a Cassegrain (monopod) modification to yield sidelobes less than -30 dB; but that degree of improvement is likely possible using the present reflector tolerances and with careful engineering of the subreflector size and taper. Recent results with offset fed reflector antennas indicate that far better sidelobe structures can be obtained by these configurations at the possible expense of some polarization deterioration. This is an issue that must be considered further should the decision be taken to seek very low sidelobe patterns.

Figures 2 and 3 show the plots of the calculations made by Fante for both polarizations of: (1) The Cassegrain-Monopod case; and (2) the best possible case attainable with the existing system having optimum dish illumination with no blockage. The two cases are compared with the patterns of the original antenna, obtained from RADC/DCCT. Figure 2 is a comparison of the vertical polarization patterns while Figure 3 compares the horizontal polarization patterns.

Note that to the main beam there is little advantage to using the Cassegrain system, as the sidelobe level remains high; however, beyond  $\pm 10^\circ$  a distinct advantage is obtained as the sidelobes are reduced considerably.

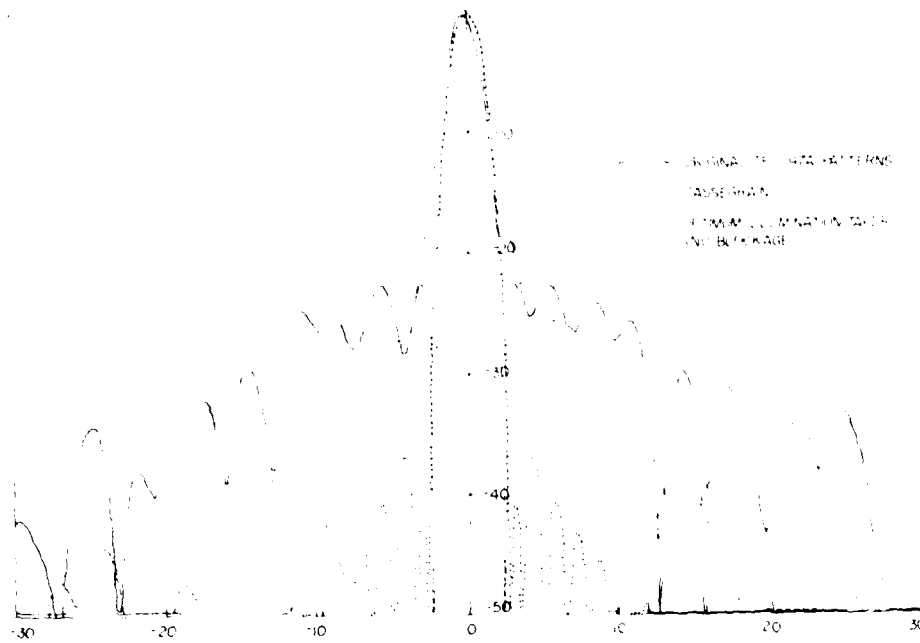


Figure 2. Comparison of the Original AN/TRC-97A Patterns With Ronald L. Fante's Calculations (Vertical polarization)

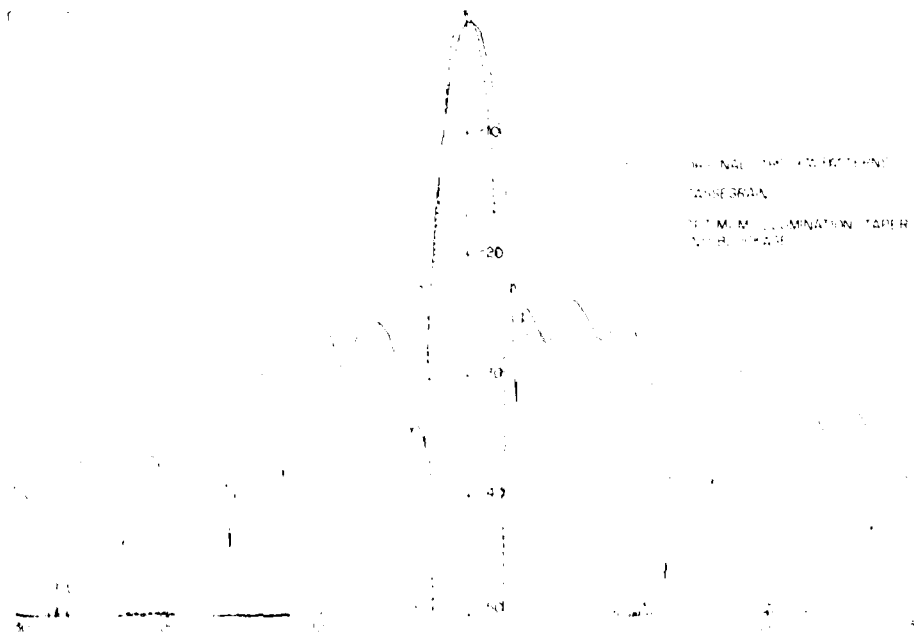


Figure 3. Comparison of the Original AN/TRC-97A Patterns With Ronald L. Fante's Calculations (Horizontal polarization)

## I. EXPERIMENTAL INVESTIGATION OF A COMPROMISE ALTERNATIVE

It is shown in the Appendices that changing the dish illumination of the existing AN FRC-97 feed would not reduce the near-in sidelobes because of the dominant blockage condition. However, since the most critical aspect of the system is the azimuth plane sidelobe structure, a possible compromise solution is to reroute the existing waveguide runs and change the strut assembly to improve the sidelobes in the azimuth plane without changing the average sidelobe level in the other planes. An experimental investigation was initiated to evaluate this alternative.

The modification consisted of removing the struts from the horizontal plane and connecting them at a  $45^\circ$  angle from the horizontal plane (Figures 1 and 4). In addition, the waveguide runs were rerouted from the vertical plane to the horizontal plane. One feed now originates at  $0^\circ$  and the other at  $180^\circ$  on the edge of the dish. This modification resulted in changing the original feed guides to a tilt angle of  $\pm 90^\circ$  from the original feed structure. Thus, azimuth patterns now taken with horizontal polarization are comparable to the original azimuth patterns taken with vertical polarization. The vertical patterns are also opposite in polarization from the originals.

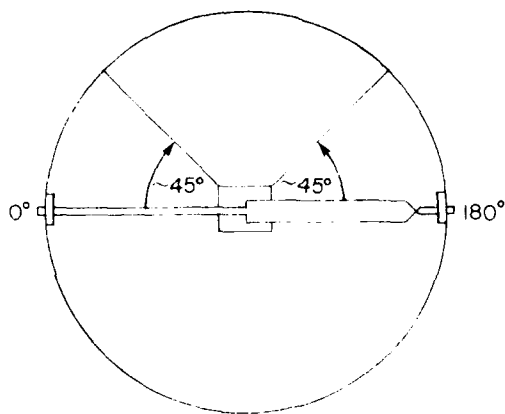


Figure 4. Modified Feedhorn and Waveguide Assembly

Principal plane patterns were taken for both polarizations by the modified feed structure and compared with the patterns sent to us by DCCF of the original feed.

As noted earlier, the polarization for equivalent horn patterns between the original and modified patterns differ by  $90^\circ$  due to the switchover of the feed horns and the  $90^\circ$  rotation of the horns. The patterns taken with the true structure set at

the original polarization. The detector is not sensitive to the polarization of the scattered wave, so the scattered wave polarization is not important. The scattered wave polarization is assumed to be unpolarized.

The scattered wave polarization is assumed to be unpolarized. The scattered wave polarization is assumed to be unpolarized. The scattered wave polarization is assumed to be unpolarized.

During this modification, the angles were not changed. The scattered wave polarization is assumed to be unpolarized. The scattered wave polarization is assumed to be unpolarized. The scattered wave polarization is assumed to be unpolarized.

Figures 6 and 7 show the patterns taken at 4.7 GHz for vertical and horizontal polarizations respectively. The solid line patterns are the scattered wave polarization patterns while the dashed line patterns are the original wave polarization patterns.

Figures 8 and 9 are patterns taken at 4.7 GHz for vertical and horizontal polarizations respectively. Again the solid line patterns are the scattered wave polarization patterns while the dashed lines are the original wave polarization patterns.

Figures 10 and 11 are the patterns for the scattered wave polarization patterns for vertical and horizontal polarizations respectively. The solid line patterns are the scattered wave polarization patterns while the dashed lines are the original wave polarization patterns.

In all cases the scattered wave polarization patterns are shown. The scattered wave polarization patterns are shown. The scattered wave polarization patterns are shown.

In addition to the original wave polarization patterns, the scattered wave polarization patterns are shown. The scattered wave polarization patterns are shown. The scattered wave polarization patterns are shown.

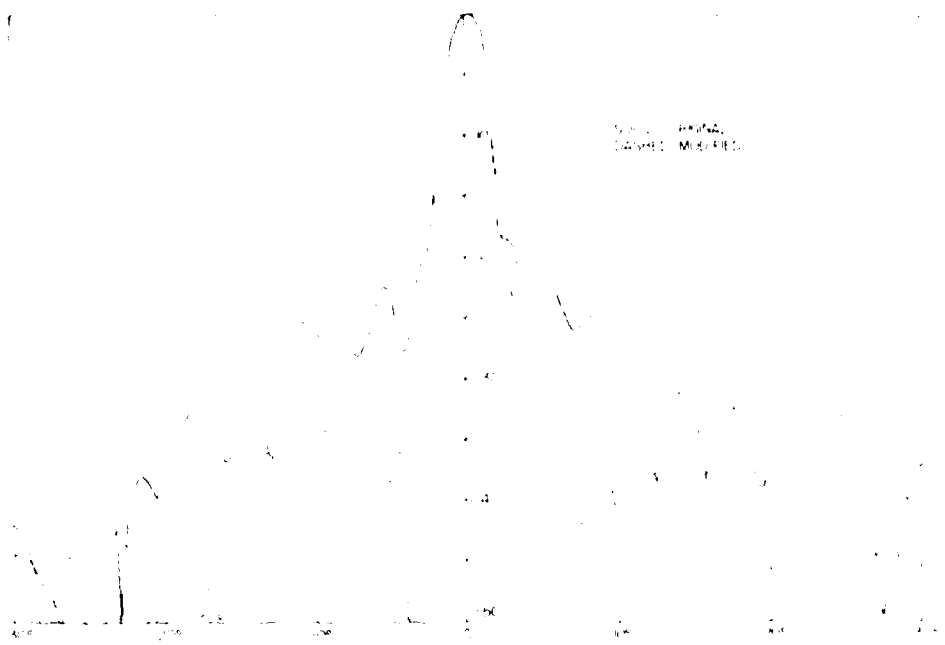


Figure 5. Comparison of the Original AN TRC-97A Patterns With the Modified Feed Structure Patterns [Vertical polarization (4.7 GHz)]

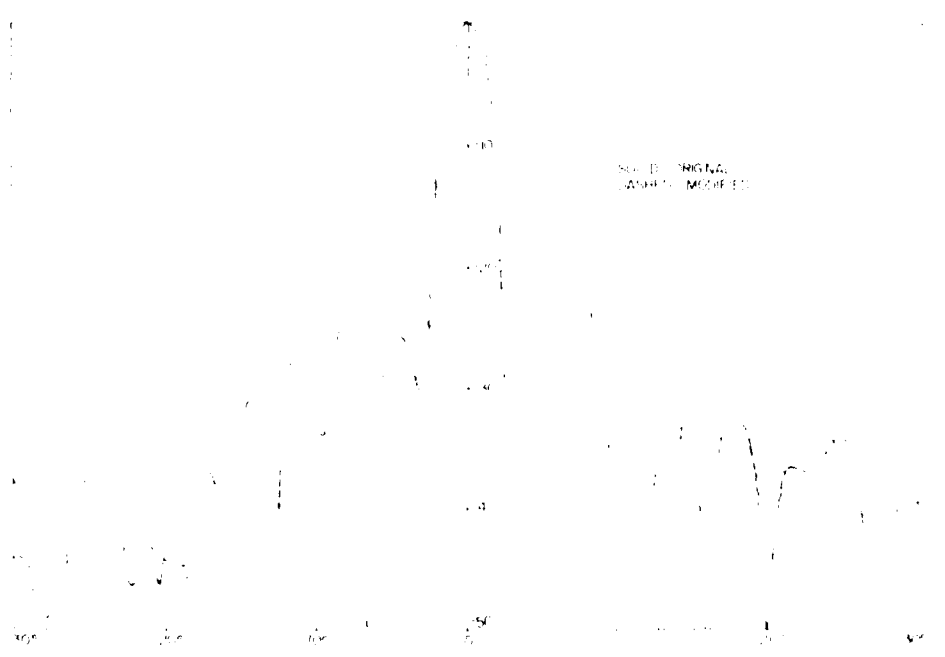


Figure 6. Comparison of the Original AN TRC-97A Patterns With the Modified Feed Structure Patterns [Horizontal polarization (4.7 GHz)]



Figure 7. Comparison of the Original AN/TRC-97A Patterns With the Modified Feed Structure Patterns [Vertical polarization (4.5 GHz)]

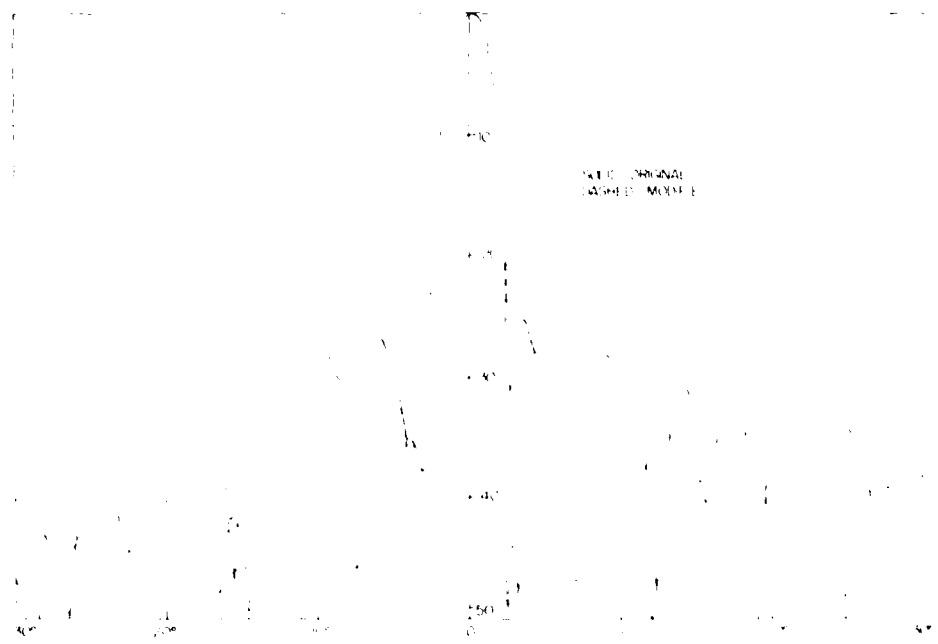


Figure 8. Comparison of the Original AN/TRC-97A Patterns With the Modified Feed Structure Patterns [Horizontal polarization (4.5 GHz)]

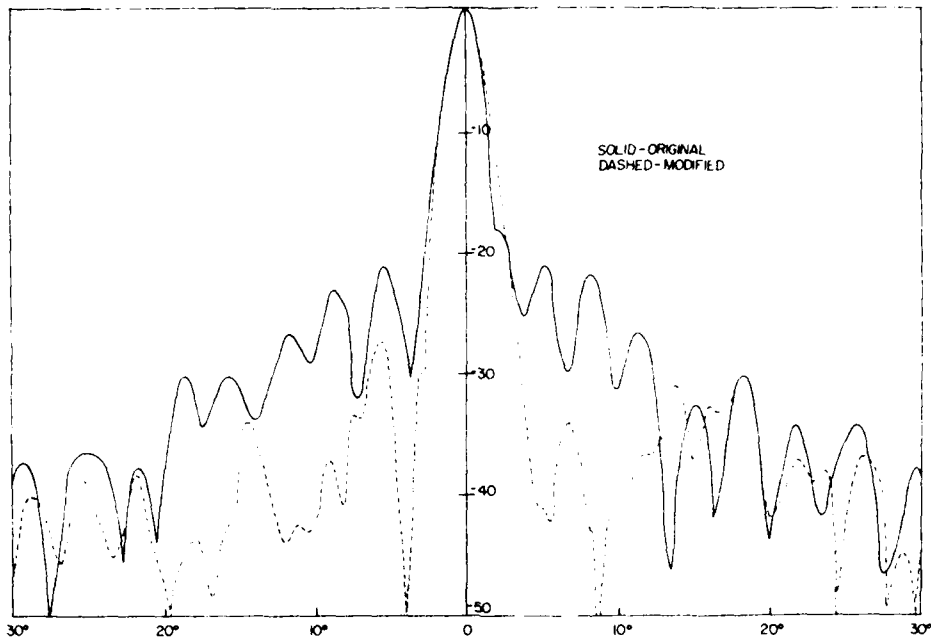


Figure 9. Comparison of the Original AN/TRC-97A Patterns With the Modified Feed Structure Patterns [Vertical polarization (4.9 GHz)]

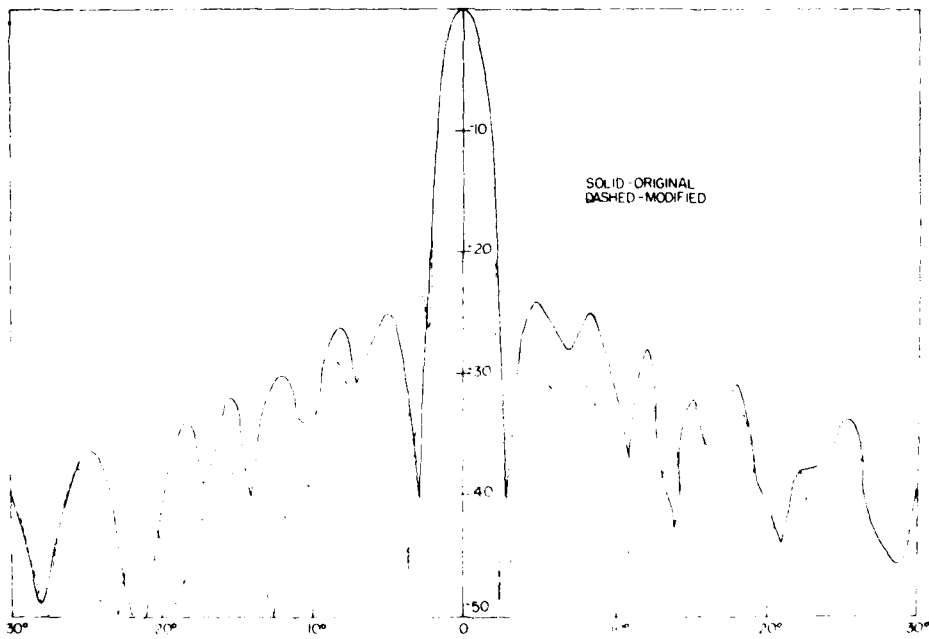


Figure 10. Comparison of the Original AN/TRC-97A Patterns With the Modified Feed Structure Patterns [Horizontal polarization (4.9 GHz)]

## 5. CONCLUSIONS

It is apparent from Ronald L. Fante's calculations and these measurements that no simple solution exists that will result in reduction in the sidelobe level of the AN/TRC-97A antenna beyond -30 dB. To achieve an appreciable improvement over the existing waveguide-feed combination an offset fed system should be considered. (See for instance RADC Report TR-77-313 entitled "ECCM Antenna Development" by RCA and RADC Report TR-77-2204, "Design of Parabolic Cylinder Reflector System with Low Sidelobes", R. L. Fante.)

Another alternative that would yield lower sidelobes than the existing feed structure in the azimuth plane, but cause some degradation in the elevation plane, would be to relocate the feed structure as in Figure 4 of the experimental work. This results in a sidelobe decrease of approximately 10 dB in the main beam area of the azimuth plane patterns ( $\pm 10^\circ$ ) and a sidelobe improvement of about 7 dB beyond  $\pm 10^\circ$ .

## Appendix A

### A Study of the Effect of Feed Blockage On The AN/TRC-97A Antenna

We have studied the effect of feed blockage on the performance of the AN/TRC-97A antenna. A drawing of the front view of this antenna is shown in Figure A1. In the absence of any blockage the field radiated by this antenna can be written as

$$E_{\theta}(\theta, \phi) = \int_0^{2\pi} \int_0^{R_0} r dr f(r) \exp \left\{ i k r \sin \theta \cos (\phi - \phi_0) \right\} \\ \pi R_0^2 \int_0^1 ds f(s^{1/2}) J_0(K R_0 \sin \theta s^{1/2}) \quad (A1)$$

where  $R_0 = 4$  ft is the radius of the parabolic reflector,  $f(r)$  is the aperture taper and  $J_0(\mu)$  is a Bessel function. Also  $k = 2\pi/\lambda$ ,  $\lambda = 2.51$  inch.

In the realistic system there is blockage due to the struts, the waveguides, and the feed assembly. By using data in the Radar Cross Section Handbook<sup>1</sup> we have calculated the effective blockage width (for  $\lambda = 2.51$  in.) of the waveguides and the struts. These are summarized in Table A1. The blockage due to the feed assembly has been approximated by a circular blockage region of radius  $R_1$ . This equivalent model is shown in Figure A2.

1. Radar Cross Section Handbook, George Ruck, Ed., Plenum Press, (1970) (Chapter 4).



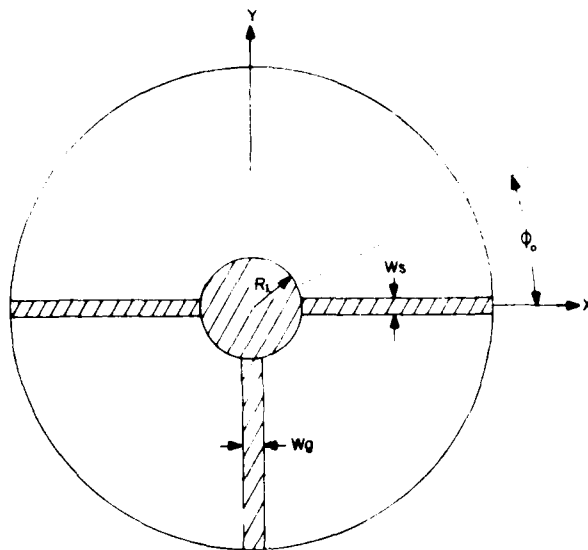


Figure A2. Equivalent Model for Blockage by Feed, Waveguides, and Struts

If  $f(r)$  is relatively constant over  $0 \leq r \leq R_1$  we can approximate  $f(r) = 1$  in the second term in Eq. (A2). Upon performing the integrals we then get

$$\begin{aligned}
 \epsilon_1(\theta, \frac{\pi}{2}) - \epsilon_0(\theta, \frac{\pi}{2}) &= 2\pi R_1^2 \frac{J_1(kR_1 \sin \theta)}{kR_1 \sin \theta} \\
 &- 0.437 \pi R_0 W_s \frac{\sin \left( \frac{k W_s}{2} \sin \theta \right)}{k W_s \sin \theta} \\
 &- W_g \int_{-R_0}^{R_0} dy f(y) e^{j k y \sin \theta} \quad (A3)
 \end{aligned}$$

where the values for  $W_1$  and  $W_2$  are those in Table VI appropriate for the polarization chosen. Also,  $J_1(x)$  is the Bessel function of order one and  $\sin^{-1} x = \sin^{-1} x$ . Similarly for  $\theta = 0$ , we get

$$\begin{aligned}
 \epsilon_1(\theta, 0) - \epsilon_0(\theta, 0) &= \pi R_1^2 \frac{J_1(kR_1 \sin \theta)}{kR_1 \sin \theta} \\
 &- 0.218 \pi R_0 W_s \frac{\sin \left( \frac{k W_s}{2} \sin \theta \right)}{k W_s \sin \theta} \quad (A4)
 \end{aligned}$$

In writing Eq. (A4) we have ignored the effect of strut blockage in the  $\phi = 0^\circ$  plane, because it has the same beamwidth as the unblocked pattern.

Equations (A3) and (A4) have been evaluated numerically and the results are shown in Figures A3 through A6. Also shown on Figures A3 through A6 is measured data.<sup>3</sup> Note that the theory predicts roughly the same blockage sidelobe levels as are measured.

In Figure A7 we show the calculated pattern [using Eq. A1] for the case when all blockage is removed, but the illumination on the dish has the same taper  $f(r)$  as the present AN/TRC-97A. In Figure A7 we also show the radiation pattern which would be obtained if the only blockage were a 5-in. diameter<sup>2</sup> circular region at the center of the aperture. This is typical of the type of blockage which would be present if the illumination were produced using a dielectric-supported subreflector.

The sidelobes shown in Figure A7, for the case of the 5-in. diameter circular blockage, are not improved significantly by reducing the edge taper on the reflector. This is evident from Figures A8a and A8b, where we compare the radiation pattern of the reflector (with 5-in. and 10-in. diameter circular blockage) for the case of -12 dB edge illumination with -26 dB edge illumination.

We have also calculated the residual sidelobe levels which are produced by tolerance errors in the construction of the AN/TRC-97A reflector. The specified rms surface tolerance is 1.16 in., but the lateral correlation length is unknown. The average sidelobe level at  $\theta$  due to tolerance errors is<sup>3</sup>

$$SL \approx \frac{4 k^2 a^2 \delta^2}{R_0^2} \exp \left( - \frac{k^2 a^2 \sin^2 \theta}{4} \right) \cos^4 \left( \frac{\theta}{2} \right) \quad (A5)$$

where  $\delta$  is the rms surface error and  $a$  is the surface-error correlation length. The worst-case sidelobes occur for a  $2/k \sin \theta$ . We then get

$$(SL)_{\text{WORST}} = \frac{5.89 \delta^2 \cos^4 \left( \frac{\theta}{2} \right)}{R^2 \sin^2 \theta} \quad (A6)$$

In Figure 9 we show the worst-case error sidelobes, along with those for surface correlation lengths of 1/4 in., 1 in., 4 in., and 8 inches. Even for worst-case correlations the error sidelobes of the AN/TRC-97A reflector will be below -40 dB for  $\theta > 13^\circ$ .

2. RADC-TR-77-369, by R. L. Fante, October 1977.

3. RADC-TR-73-2, Rome Research Corp., 31 March 1973.

If the diameter of the feed were 10-in. instead of 5 in. the blockage sidelobe would be as shown in Figure A8b.

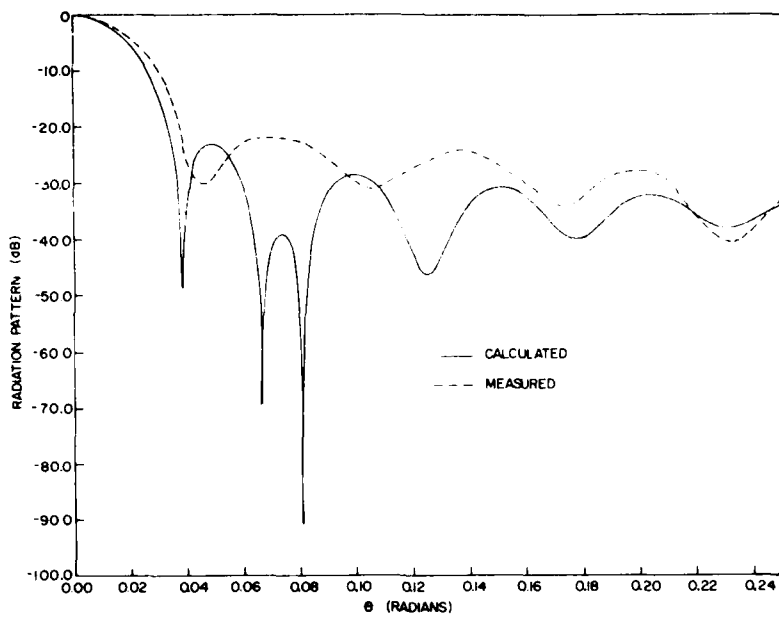


Figure A3. Pattern for Horizontal Polarization in the Horizontal Plane

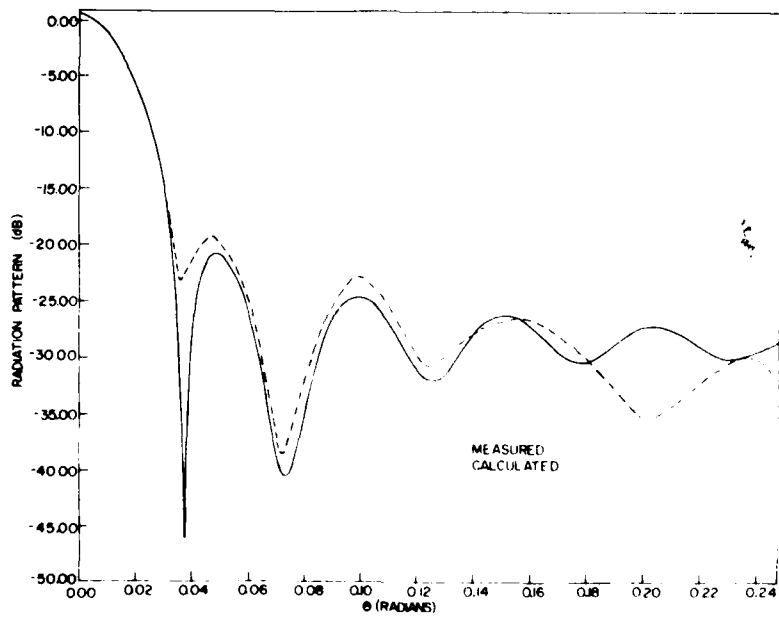


Figure A4. Pattern for Horizontal Polarization in the Vertical Plane

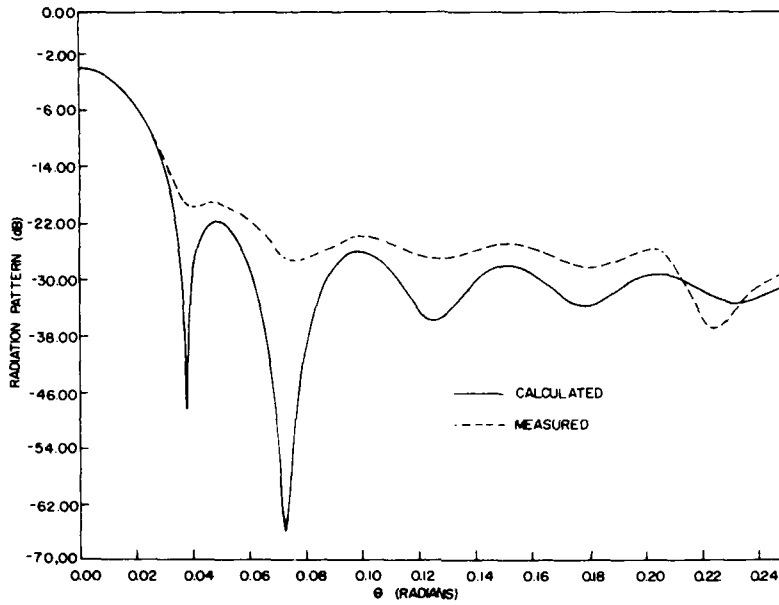


Figure A5. Pattern for Vertical Polarization in the Horizontal Plane

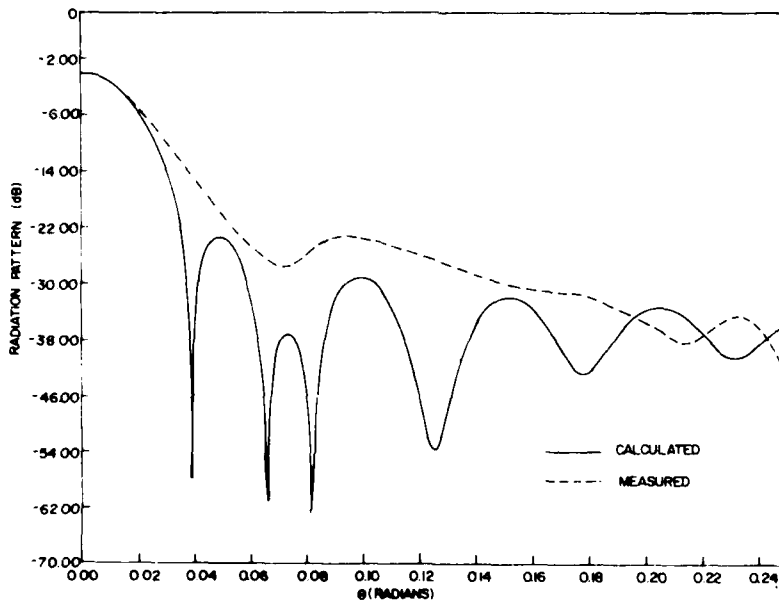


Figure A6. Pattern for Vertical Polarization in the Vertical Plane

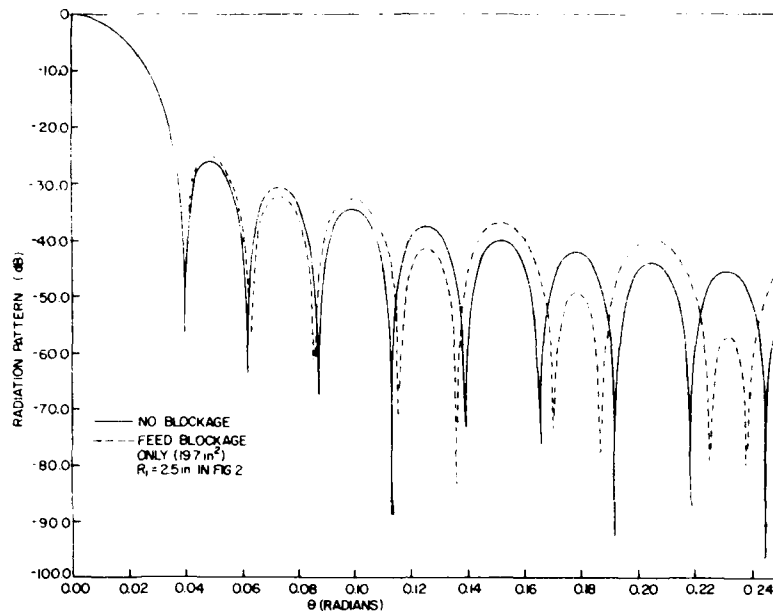


Figure A7. Radiation Pattern of the AN/TRC-97A Reflector (12 dB Edge Illumination)

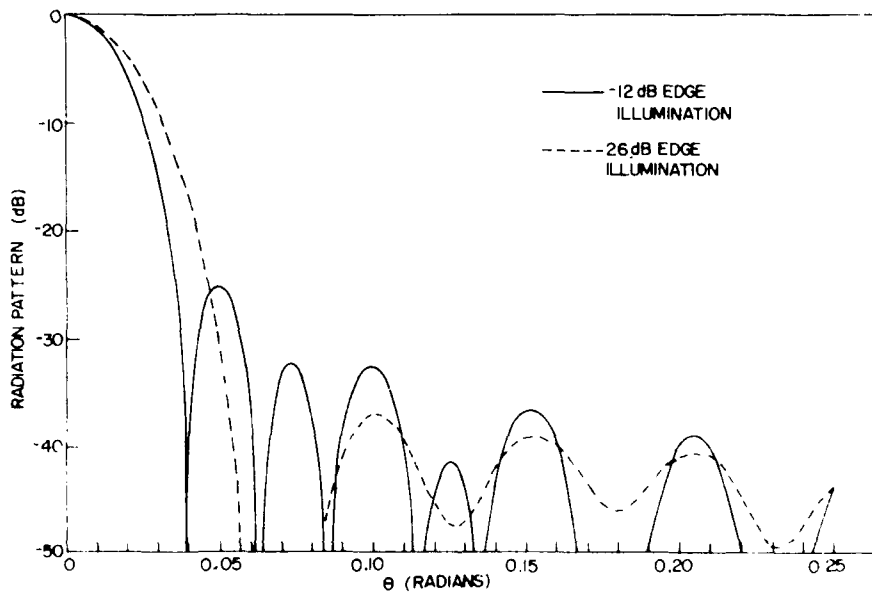


Figure A8a. Radiation Pattern of the AN/TRC-97A Reflector With Blockage by 5-in. Diameter Circular Feed for Two Different Edge Illuminations. The -12 dB represents the present TRC-97A

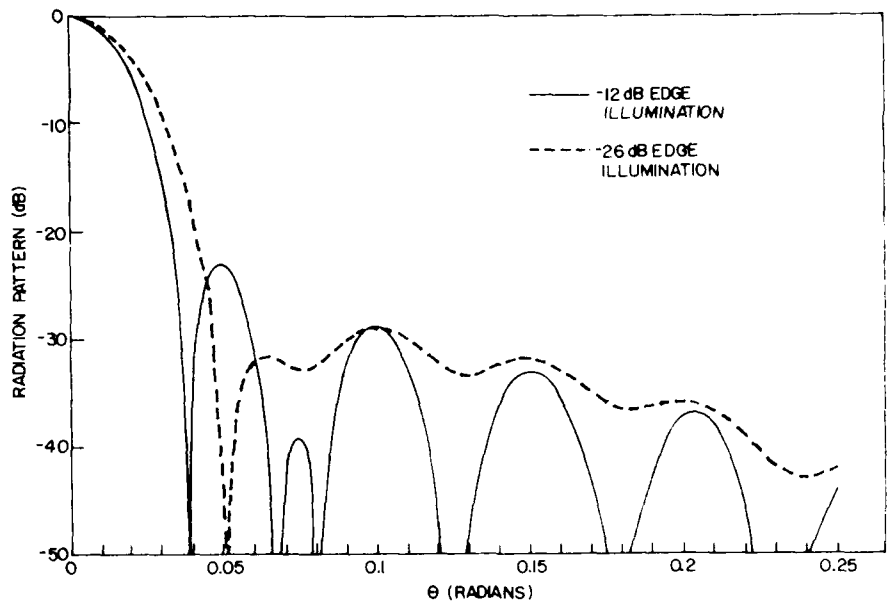


Figure A8b. Radiation Pattern of the AN/TRC-97A Reflector With Blockage by 10-in. Diameter Circular Feed for Two Different Edge Illuminations

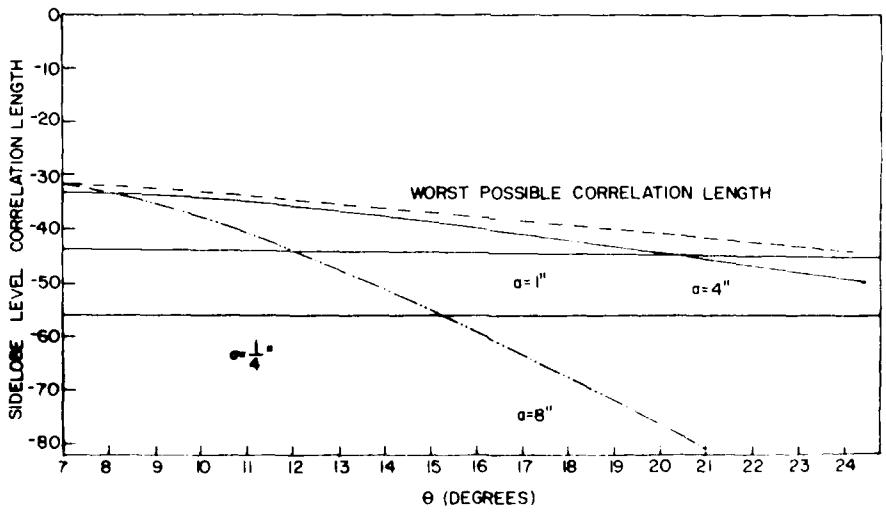


Figure A9. Average Sidelobe Levels Due to Reflector Tolerance Errors for Different Correlation Lengths, (a)

### Conclusions

The blockage due to near-in sidelobe levels of more than 30 dB is not completely negligible. It is about 1% for  $\theta = 10^\circ$  and 0.1% for  $\theta = 20^\circ$ . The sidelobe level due to the near-in sidelobe is about 10 dB higher than the level due to the near-in sidelobe. The sidelobe level due to the near-in sidelobe would be about -40 dB if the near-in sidelobe level were higher. This conclusion would not be altered if a more highly tapered edge illumination is used, as is clear from Figure A9.

Because the correlation length of surface tolerance errors is unknown, we are unable to calculate the error sidelobe. However, in any case they are certainly no worse than predicted by the dashed curve on Figure A9, and probably much better because our best guess, based on a cursory visual inspection, is that the correlation length is about 6 to 10 inches.

### Recommendations

The present AN/TRC-97A antenna configuration will have near-in sidelobe levels of order of -30 dB for higher  $\theta$ ; changing the dish illumination will not affect this conclusion because the sidelobe are due to blockage by the feed and its supports.

The near-in sidelobe could be reduced to roughly -40 dB by removing all blockage except a centrally located feed of area  $20 \text{ in.}^2$  or less and increasing the amount of taper on the dish illumination.

Sidelobe of order of -30 dB or lower might possibly be achieved if surface errors are reduced. However, because of mechanical tolerance errors, it is unlikely that the sidelobe would be less than -30 dB for  $\theta > 10^\circ$ , as is clear from Figure A9.

### References

This feed could be a heliostat-supported collector for power transmission to the dish.

## Appendix B

### Analysis of the Effect of Subreflector Blockage on the Radiation Pattern of a Cassegrain Modification to the AN/TRC-97A Antenna

#### BL. ANALYSIS

In this appendix, we will calculate the sidelobe levels for the AN/TRC-97A antenna when it is fed in an optimally designed Cassegrain configuration. The minimum blockage design corresponds to the case when the shadow cast upon the main reflector by the feed is exactly equal<sup>4</sup> to the shadow cast by the hyperboloidal subreflector. Upon referring to Figure B1 we see that this condition is expressed via the equations

$$\tan \theta = \frac{D_B}{2S} \quad (B1)$$

$$\frac{D_B}{F} = \frac{d_m}{F_c} \quad (B2)$$

where  $D_B$  is the diameter of the hyperboloidal subreflector,  $\theta$  is the angle subtended at the feed by the subreflector edge,  $d_m$  is the feedhorn diameter,  $F_c$  is the distance between the two foci of the hyperboloid (the feed horn is at one of the

<sup>4</sup>Hannan, P.W. (1961) IEEE Trans. Antennas Propag. AP-9:140-153.



where  $\lambda$  is the signal wavelength. Equation (B3) is valid in the magnetic plane of the horn, and is not quite correct in the electric plane.

If we combine Eqs. (B1) and (B2), along with the definition of S we obtain

$$\tan \phi = \frac{L_B^2}{2d_m F - D_B^2 \cot \theta} \quad (B4)$$

Finally, using Eq. (B3) to express  $d_m$  in terms of  $\phi$  we get

$$D_B = \left[ \frac{3.48 \lambda F \left( \frac{\tan \phi}{\phi} \right)}{1 + \tan \phi \cot \theta} \right]^{-1/2} \quad (B5)$$

Equation (B5) expresses the minimum possible blockage diameter in terms of the angle  $\theta$  subtended at the focus by the main reflector edge, and the angle  $\phi$  subtended at the feed by the subreflector (for the case when the subreflector edge illumination is -20 dB). We also note that once  $\theta$  and  $\phi$  are chosen the subreflector eccentricity,  $e$ , follows immediately via

$$e = \frac{\sin \frac{1}{2} (\theta + \phi)}{\sin \frac{1}{2} (\theta - \phi)} \quad (B6)$$

Also, once  $\phi$  is specified the diameter,  $d_m$ , of the feed horn is given by Eq. (B3).

The AN/TRC-97A has a focal length of approximately 3.2 ft, a wavelength,  $\lambda$ , of 2.51 in. and  $\theta \approx 64^\circ$ . Using these values we obtain the results shown in Table B1.

Table B1.

$\phi$ (degrees)	$D_B$ (ft)	$d_m$ (ft)	$e$	$s$ (ft)	$\frac{2d_m^2}{\lambda}$ (ft)
20	1.43	1.04	1.78	1.81	10.35
30	1.41	0.695	2.5	1.11	4.62
40	1.40	0.521	3.79	0.752	2.6
50	1.41	0.417	6.88	0.54	1.66
60	1.44	0.348	25.3	0.40	1.16

From Table B1, we see that the minimum possible subreflector diameter,  $D_B$ , is approximately 1.4 feet. This result is relatively insensitive to the subreflector eccentricity,  $e$ . From the last two columns of Table B1 we also note that the

distance,  $\delta$ , from the feed to the subreflector is generally less than  $(2 d_m^2 / \lambda)$ , so that the subreflector is not quite in the Fraunhofer zone of the feed. It is most nearly in the Fraunhofer zone when the feed is close (high eccentricity to the subreflector, as is evident from Table B1).

At this point we shall calculate the effect of the subreflector blockage on the radiation pattern of the main reflector, for the case when the main reflector has a -20 dB edge taper. This result is shown in Figure B2. We observe from this figure that the feed blockage (caused by the hyperboloidal subreflector) produces near-in sidelobes which are greater than -30 dB, although the far-out (angles greater than  $9.7^\circ$ ) sidelobes are below -40 dB.

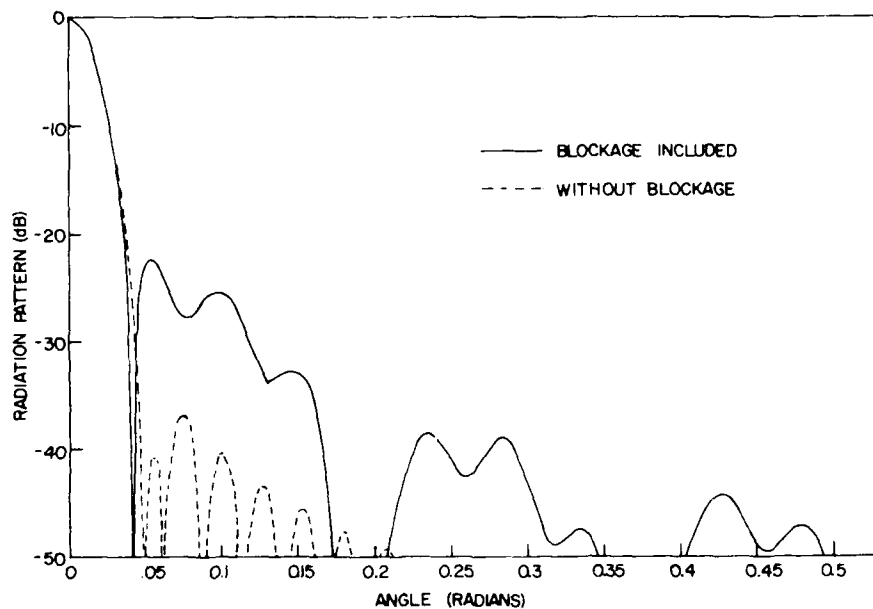


Figure B2. AN/TRC-97A Radiation Pattern With Minimum Blockage Cassegrain Feed and -20 dB Edge Taper

One might ask if we do any better by "backing-off" to a -14 dB edge taper, rather than a -20 dB taper. In this case Eq. (B3) is replaced by  $\phi_{-13} \approx 1.4 \lambda / d_m$  and we then find that the minimum possible subreflector diameter is  $D_B = 1.19$  feet. However, when we calculate the radiation pattern of the AN/TRC-97A reflector with this blockage and a -14 dB edge illumination we again get near-in sidelobes greater than -30 dB (in fact the first sidelobe is roughly -22 dB), as is evident from Figure B3.

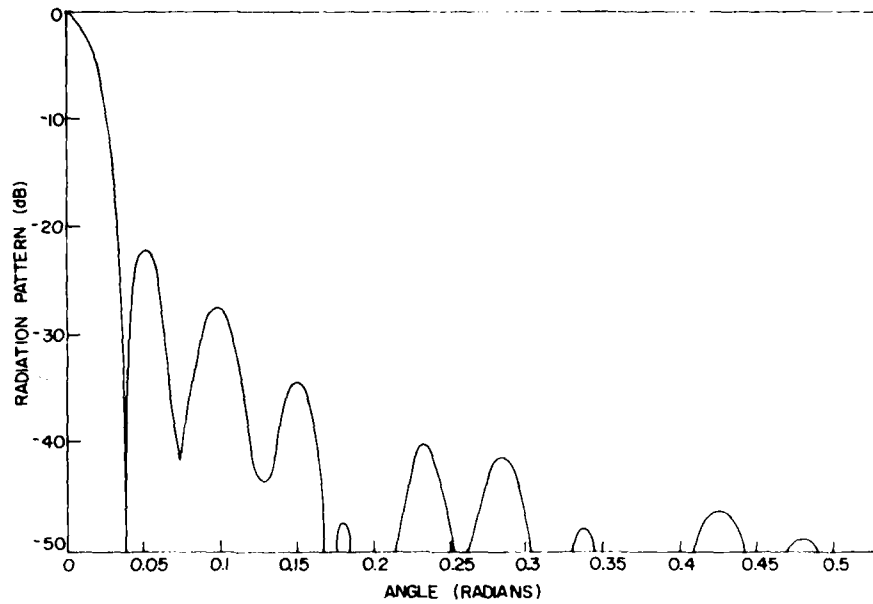


Figure B3. AN/TRC-97A Radiation Pattern With Minimum Blockage Cassegrain Feed and -14 dB Edge Taper

## B2. CONCLUSION AND RECOMMENDATION

Because of subreflector blockage it does not appear possible to design a Cassegrain-subreflector modification to the AN/TRC-97A which will yield a system radiation pattern with all sidelobes less than -30 dB. If this performance is desired an offset fed system seems to be the simplest alternative.

### B2.1 Design of the Conical Feed Horn

If we should choose to build the Cassegrain system we will need a feed-horn design, as shown below in Figure B4.

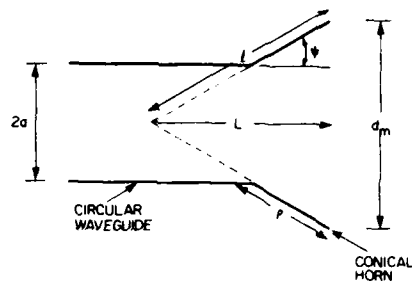


Figure B4.

If we desire only the  $TE_{11}$  mode in the waveguide feeding the horn we must choose "a" such that

$$2.61a < \lambda < 3.41a, \quad (B7)$$

because the cutoff wavelength  $\lambda_c$  of the  $TE_{11}$  is  $3.41a$  and that of the next mode ( $TM_{01}$ ) is  $2.61a$ . If we choose  $3a = \lambda$  we have

$$2a = \frac{2\lambda}{3} = \frac{(2.51)^2}{3} = 1.67 \text{ inch.} \quad (B8)$$

The dimensions  $L$  and  $\rho$  are determined from the equations given by King (1950) Proc. IRE, 38:249-51. These are

$$\frac{L}{\lambda} = 0.3 \frac{d_m}{\lambda} \quad (B9)$$

$$\frac{\rho}{\lambda} = 0.3 \left[ 1 + \left( \frac{d_m}{\lambda} \right)^2 \right] \quad (B10)$$

and the horn angle  $\psi$  is determined via

$$\cos \psi = \frac{\left( \frac{d_m}{\lambda} \right)^2}{\left[ 1 + \left( \frac{d_m}{\lambda} \right)^2 \right]} \quad (B11)$$

$$\rho = 0.3 \lambda \left[ 1 + \left( \frac{d_m}{\lambda} \right)^2 \right] = \frac{a}{\sin \psi}. \quad (B12)$$

As an example, consider the design for the case when  $e = 6.88$  in Table B1. In this case  $(d_m/\lambda) = 1.99$  so that

$$\left(\frac{L}{\lambda}\right) = 1.19,$$

$$\frac{c}{\lambda} = 1.49,$$

$$\cos \psi = 0.798,$$

$$\psi = 37^\circ,$$

and

$$\left(\frac{\rho}{\lambda}\right) = 0.936.$$

#### B2.2 Example of Hyperboloidal Subreflector Design

The hyperboloid is designed as shown in Figure B5.

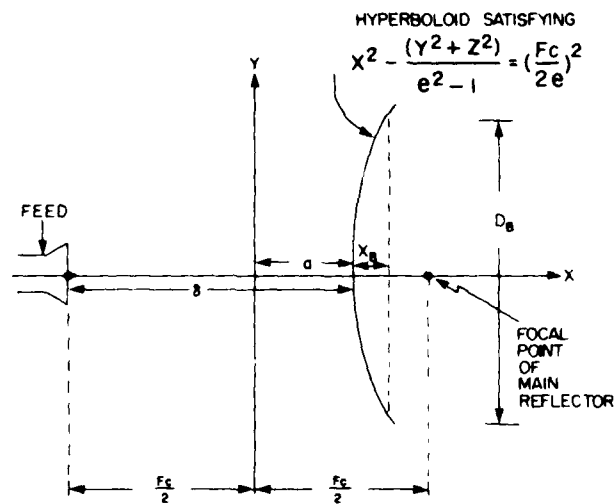


Figure B5

In Figure B5,  $a = (F_c/2e) \delta = (F_c/2) + a$  and

$$X_B = \left[ \left( \frac{F_c}{2e} \right)^2 + \frac{D_B^2}{4(e^2 - 1)} \right]^{1/2}$$

If we choose to design the system in Table B1 for which  $e = 6.85$  we have  
 $F_c = 0.946$  ft,  $D_B = 1.41$  ft,  $a = 0.0687$  ft,  $\delta = 0.541$  ft, and  $X_B = 0.124$  feet.



*MISSION*  
*of*  
*Rome Air Development Center*

*RADC plans and executes research, development, test and selected acquisition programs in support of Command, Control Communications and Intelligence (C<sup>3</sup>I) activities. Technical and engineering support within areas of technical competence is provided to ESD Program Offices (POs) and other ESD elements. The principal technical mission areas are communications, electromagnetic guidance and control, surveillance of ground and aerospace objects, intelligence data collection and handling, information system technology, ionospheric propagation, solid state sciences, microwave physics and electronic reliability, maintainability and compatibility.*

LMED  
-18